

# Quantification of particle shape by an automated image analysis system: a case study in natural sediment samples from extreme climates

Young Ji Joo<sup>1\*</sup>, Anastasia M. Soreghan<sup>2</sup>, Megan E. Elwood Madden<sup>2</sup>, and Gerilyn S. Soreghan<sup>2</sup>

<sup>1</sup>Division of Polar Paleoenvironments, Korea Polar Research Institute, Incheon 21990, Republic of Korea

<sup>2</sup>School of Geology and Geophysics, University of Oklahoma, Norman, OK 73010, U.S.A.

**ABSTRACT:** Sediment particle shape and microtexture are key parameters utilized for characterizing sediment transport and weathering (both physical and chemical) processes, which in turn are governed by environmental conditions such as climate. Assessing particle shape often involves either qualitative descriptors or time-consuming measurements of shape parameters by a human operator. This study employs a state-of-the-art, quantitative shape analysis instrument known as the “Morphologi G3” from Malvern Instruments, an automated microscope system capable of determining quantitative shape parameters via static image analysis of > 1000 particles in less than two hours. This instrument captures 2D projected images of particles and provides information on grain size measurements such as circle-equivalent diameter, length, width, perimeter, and area, as well as shape parameters such as circularity and convexity. As a case study, we conducted analyses on mud- and sand-sized particles collected from fluvial/alluvial systems of end-member climates to assess variations in sediment particle morphology potentially related to climate and/or transport distance and processes. Sediment samples were collected from fluvial systems in four contrasting climates: hot-arid (south-eastern California, USA), hot-humid (eastern Puerto Rico), glacial-arid (proglacial stream of the Dry Valleys, Antarctica), and glacial-humid (Austerdalen proglacial stream, Norway). Results provide quantitative constraints on shape differences that relate to climate and transport, even for very fine-grained sand and mud size fractions. Comparison of the circularity of sediment particles from the four end-member climates indicates that the very fine sand fractions reflect differential physical abrasion and transport processes, whereas the morphology of the mud fraction seemingly imprints chemical weathering processes. We conclude that this new technique has great potential to further document impacts of climate on particle shape with applications to both modern and deep-time depositional systems.

**Key words:** particle shape, morphology, image analysis, glacial sediment, circularity, convexity

Manuscript received May 8, 2018; Manuscript accepted May 26, 2018

## 1. INTRODUCTION

Sediment particle morphology observations based on microscopic analyses have long been used to document weathering signals and interpret transport processes, and thus reconstruct depositional environments (see Vos et al., 2014 for review). While some particle morphology features can be produced under a range of different conditions (Margolis and Krinsley, 1974; Mahaney, 1995, 2002), a few extreme environments

such as wet-based glacial systems are known to produce unique suites of particle surface microtextures (e.g., Mahaney, 2002; Smith et al., 2018). Scanning electron microscopy (SEM) allows direct, three-dimensional observation of particles with great depth of focus and magnification; however, SEM analyses are often prohibitively time-consuming and expensive for obtaining a reliable dataset from a sufficient number of grains. This study employs a new, time-efficient method to determine particle morphology using a Morphologi G3 from Malvern Instruments Limited. The instrument characterizes and quantifies morphology of sediment particles, which has the potential to significantly impact (paleo) climate interpretation. Recent work by Becker et al. (2018) introduced a novel, Morphologi G3-based method for identifying and counting sand-sized, ice-rafted debris, which is a proxy of enhanced sediment transport by icebergs and sea ice,

### \*Corresponding author:

Young Ji Joo  
Division of Polar Paleoenvironments, Korea Polar Research Institute,  
26 Songdomirae-ro, Incheon 21990, Republic of Korea  
Tel: +82-32-760-5386, Fax: +82-32-760-5397, E-mail: yjoo@kopri.re.kr

©The Association of Korean Geoscience Societies and Springer 2018

in marine sediments deposited during glacial/interglacial transitions.

In this study we employed automated particle image analysis to compare grain morphology metrics of natural sediments collected from fluvial systems in four end-member climates (hot-arid, hot-humid, cold-arid, and cold-humid) characterized by similar bedrock lithology and drainage basin sizes. Our purposes are 1) to test the applicability of the new instrument for environmental (climate) interpretation using sediment samples and 2) to assess particle shape differences imparted by the varying climates based on quantification of morphological parameters. We analyze sediment particles within two distinct size ranges: very fine sand (63–125  $\mu\text{m}$ ) and mud (< 63  $\mu\text{m}$ ). We focused on fine-grained sediments since these size fractions, particularly the mud component, are critical for identifying weathering signals, especially in glacial systems (Marra et al., 2014, 2017). We also compared multiple sediment samples collected along each stream transect to investigate the effects of transport distance on particle shapes.

## 2. METHODS

### 2.1. Sample Collection

Sediment samples from four end-member climates were selected for the automated image analysis using the Morphologi G3. Sampling sites were chosen based on similarities in drainage basin size and bedrock lithology in order to highlight effects of the different climates (Table 1). The four end-member field areas are 1) a hot-arid alluvial system in the Anza Borrego Desert (ABD) of southern California, 2) a hot-humid fluvial system in eastern Puerto Rico, 3) a cold-humid proglacial system in Norway, and 4) a cold-arid proglacial system in the McMurdo Dry Valleys (MDV), Antarctica (Fig. 1). In the Anza Borrego site, the alluvial sediment undergoes only limited fluvial transport during rare precipitation events sufficiently intense to generate overload flow. The role of eolian processes appears to be subordinate in the sampling site, which is located in a relatively protected “wineglass canyon” (Remeika and Lindsay, 1992) with lack of well-developed sand dunes and relatively low eolian sediment fluxes (Fig. 1a) (Joo et al., 2016). In contrast, the sediment from the main channel of Rio Guayanés of eastern

Puerto Rico (Fig. 1c) experiences vigorous fluvial transport, with relatively high discharge rate ( $\sim 2.02 \text{ m}^3/\text{s}$ ; USGS National Water Information System) in the intermontane watershed. The proglacial stream of the Austerdalen valley in Sognefjord (Norway) is fed by the Jostedal ice field and joins a stream of the Langedalen valley to flow to the Storelvi river (Figs. 1e and f). The flow is highest during the peak melting season (late summer) with the average summer rate comparable to that of the Rio Guayanés. The ephemeral, proglacial stream emanating from surficial melting of Clark Glacier in Wright Valley of the MDV flows only  $\sim 6$ –12 weeks during the brief austral summer. In the MDV, intensive easterly (from the Ross Sea) and westerly (from the polar plateau) winds, as well as winter katabatic winds from the East Antarctic Ice Sheet ( $\sim 40 \text{ m/s}$ ) promote significant eolian sediment flux (Clow et al., 1988; Doran et al., 2008; Gooseff et al., 2011).

As illustrated in Figure 1, all four sites are underlain by crystalline bedrock of granitoid compositions, and modern alluvium. The Norway site is underlain by foliated granitic gneiss (Fig. 1f), while the ABD, Puerto Rico, and MDV watersheds are underlain by non-foliated, plutonic bedrocks. Since no sedimentary strata occur in any of the sampling sites, we do not expect any of the morphological features that have been inherited from previous depositional cycles. In the MDV site, however, the valley-filling drift deposits reflect complex glacial histories, including a shift from the Oligocene wet-based glaciation to cold-based glaciation, which has been maintained since the Miocene (e.g., Lewis et al., 2006). Samples were collected along a  $\sim 6$ –16 km transect (Table 1), starting from the headwater regions, consistently targeting the fine-grained (slack-water) parts of lateral bars, typically the downstream termini of such bars. Three samples from the proximal, medial, and distal parts of each transect were analyzed to assess effects of transport distance on particle morphology.

### 2.2. Analytical Procedure

#### 2.2.1. Sediment sample preparation

We treated sediment samples collected from the natural depositional systems prior to the image analysis. Bulk sediments were first wet-sieved to separate the sample into gravel (> 2 mm), sand (63  $\mu\text{m}$ –2 mm), and mud (< 63  $\mu\text{m}$ ) fractions. The sand

**Table 1.** Sample site characteristics

Site	Climate	Bedrock lithology	MAT ( $^{\circ}\text{C}$ ) <sup>(a)</sup>	MAP (mm/y) <sup>(b)</sup>	Transect (km)
Anza Borrego, California	Hot, arid	Tonalite	23	150	6
Puerto Rico	Hot, humid	Granodiorite, metavolcanics, diorite	22	4200	15
Norway	Cold, humid	Quartz monzonite, granitic gneiss, granodiorite	4.5	1769	16
Antarctica	Cold, arid	Granitoids	–18	100	6

<sup>(a)</sup>Mean Annual Temperature; <sup>(b)</sup>Mean Annual Precipitation.

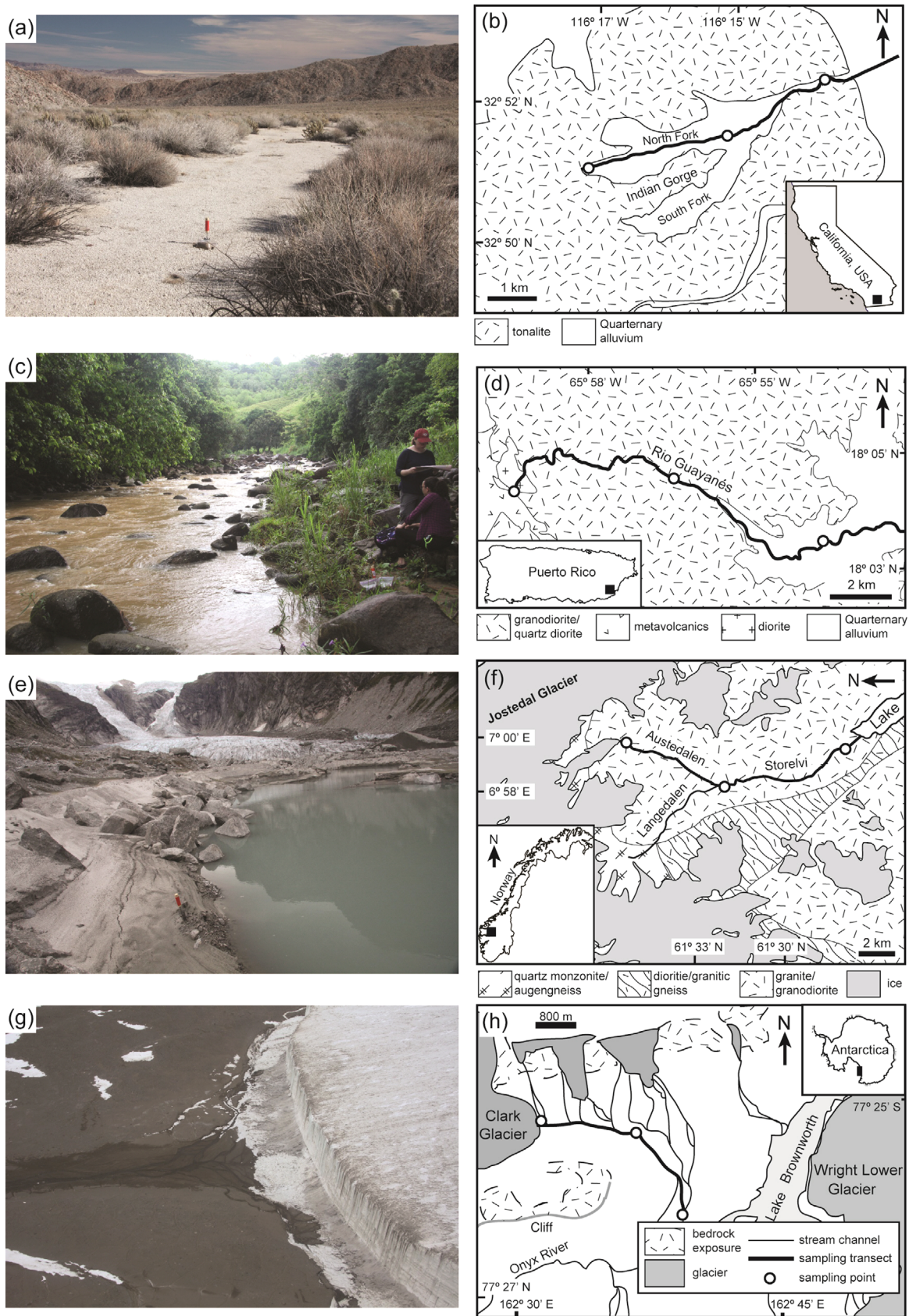


**Fig. 1.** Field photos and geologic maps of the four end-member climate localities. (a and b) Anza Borrego, California; (c and d) Puerto Rico; (e and f) Norway; (g and h) Antarctica. Geologic maps are modified after Strand (1962) (Anza Borrego), Rogers et al. (1979) (Puerto Rico), Lutro and Tveten (1996) (Norway), and Hall and Denton (2005) (Antarctica).

fraction was further sieved to isolate the very fine sand (63–125  $\mu\text{m}$ ) fraction. The mud and very fine sand fractions were treated overnight with buffered acetic acid (pH ~4.8) to remove carbonate and then with hydrogen peroxide (~30%; up to several days) to remove organic matter. Between each step, the samples were thoroughly rinsed three times with deionized water. Following the chemical treatment, samples were freeze dried and stored for analysis.

### 2.2.2. Automated image analysis

The Morphologi G3 system comprises an automated microscope bundled with a software package that allows microscope control, image collection, and post-collection analysis (e.g., statistics) (Fig. 2a). The instrument captures images of the particles loaded on a glass plate, automatically moving the “scan area”, which is a window defined by the user in the software. The instrument yields high-resolution images of particles (Fig. 2b) sufficient for analyzing shapes and, to some extent, surface features. During analysis, it also measures and calculates width, length, area, and various shape parameters describing particle morphology (Table 2) (Malvern Instruments Ltd., 2015). This study focuses on two descriptors related to the particle roundness and surface irregularities, the High Sensitivity (HS) Circularity and Convexity

(Table 2; Fig. 2c).

The first step of the image analysis on the Morphologi G3 system is to decide the method of sample dispersion onto the glass plate – the system allows for either dry or wet dispersion. For the dry method, a small amount of sample is first placed in the sample loading well and then accumulates on the large glass plate after mobilization by a short burst of pressurized nitrogen gas followed by a settling period. This process takes place within a sample dispersion cylinder to prevent possible sample loss and contamination of dust particles (Fig. 2a). Based on our experiences, this method is appropriate when the volume of the sample is relatively large. When the sample volume is very small (e.g., dust samples), it appears better to use methanol or DI water as a dispersant and, if necessary, use the smaller glass plate for dispersion of the particles (Fig. 2a). The wet sample can be loaded directly on a glass plate using an eyedropper and dried either in ambient air or in an oven (~40 °C) to completely remove the dispersant medium.

The image analysis on the Morphologi G3 is executed following a user-defined standard operating procedure (SOP), which is a collection of methods chosen for each step of the analysis. Once the user sets up an SOP for the samples, up to four samples (Fig. 2a) can be sequentially and automatically

**Table 2.** Definitions of selected particle shape parameters available in Morphologi G3 (Malvern Instruments Ltd., 2015)

Parameter	Definition
Area	Visual projected area of a particle
Aspect Ratio	Ratio of the width to the length of a particle
Perimeter	Total length of the particle boundary
Circle Equivalent (CE) Diameter	Diameter of the circle with the same area as the projected particle area
High Sensitivity (HS) Circularity	Ratio of the particle's projected area to the square of the perimeter of the particle
Convexity	Perimeter of the convex hull of the particle divided by perimeter of the particle (spikiness)
Elongation	1 – Aspect Ratio
Solidity	Particle area divided by the area enclosed by the convex hull

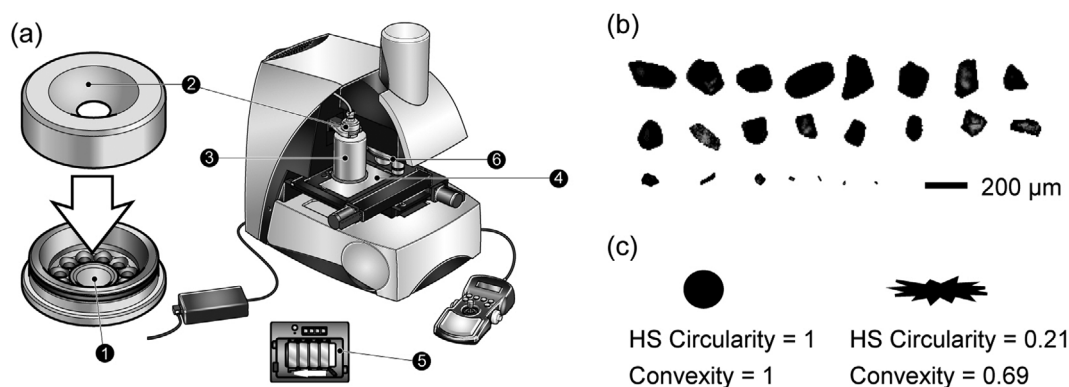


**Fig. 2.** Major components of the Morphologi G3 system (a) showing the sample loading well (1) in the sample entrainment spool (2), sample dispersion cylinder (3), which spreads particles on either a large glass plate (4) or multiple small glass slides in the sample carrier (5), and the optical unit with five different objective lenses (6) (modified after Malvern Instruments Ltd., 2015). Selected images of particles obtained using Morphologi G3 (b) and illustrative explanation of the two particle shape parameters discussed in this study (c).

analyzed. Designing an SOP includes selecting 1) the duration and strength of the pressurized air release for the dry dispersal, 2) the size of the scan area, 3) the detection threshold, and 4) the objective lens with a magnification appropriate to cover the sample particle size range (see Morphologi G3 manual by Malvern Instruments Ltd., 2015 for more details). The operator can also choose to capture particle images using multiple objective lenses and then perform “focus stacking” to yield high-resolution images of samples with broad size ranges, albeit with a significant increase in measurement time/sample. The duration of measurement depends on the scan area and the magnitude of the objective lens. For instance, the measurement time varies between less than an hour (~2000–3000 particles) and ~5–6 hours (> 100,000 particles) for the samples presented in this paper. The particle shape parameters are calculated and saved simultaneously during the image capturing process.

### 3. RESULTS AND DISCUSSIONS

#### 3.1 Fine-grained Sand

The measured HS Circularity distributions of the very fine sand fractions from all four sites illustrate clear separation with respect to the climate regimes, with overall lower HS Circularity occurring in the glacially influenced sites (Norway and Antarctica) and broader curves with higher HS Circularity in the warm-climate sites (ABD and Puerto Rico) (Fig. 3a). Considering that

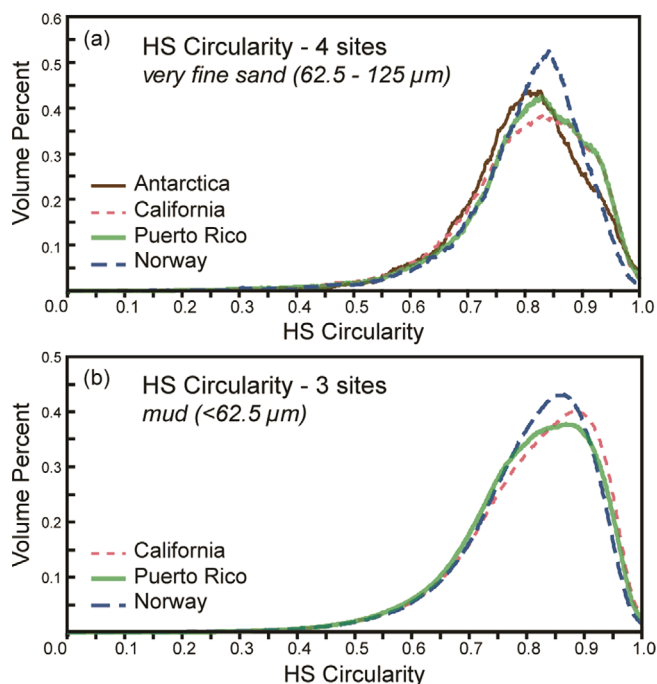


**Fig. 3.** HS Circularity of the very fine sands from all four sites (a) and the mud fractions from California, Puerto Rico, and Norway (b).

sediments comminuted beneath glaciers experience vigorous edge-to-edge grain crushing, fracturing, and attrition as observed in microscopic analyses (e.g., Evans et al., 2006; Smith et al., 2018), the lower circularity in the two proglacial systems is not unexpected. The difference between the Norway and Antarctica samples likely derives from strong climatic influences stemming from both glacial and eolian processes. With the strong winds in the MDV, the wider range of the HS Circularities of the Antarctic very fine sand can be attributed to eolian fluxes of more rounded sediment and/or wind-driven particle abrasion that produce more rounded particles.

#### 3.2. Mud-sized Grains

There is also a contrast in the particle circularities observed in the mud fractions, but this seems to be more closely associated with wet versus dry climates: HS Circularities are lower in the Puerto Rico and Norway sediments compared to the ABD samples (Fig. 3b). We interpret this as a result of a stronger degree of chemical weathering in Puerto Rico and Norway owing to their higher water availability. As it is observed in microscopic analyses (Pye and Mazzullo, 1994; Vos et al., 2014; Woronko, 2016; and references therein), intense chemical weathering generates features such as dissolution pits and crevasses, and precipitates secondary phases on particle surfaces, thus lowering particle circularity. Alternation of wetting and drying due to air temperatures and moisture levels fluctuating below and above the freezing point can further enlarge surface irregularities in the Norway site (e.g., May, 1980).

#### 3.3. Comparison of Cold-based vs. Warm-based Glacial Sites

The comparison of the measured HS Circularities from the four end-member climate systems indicates that 1) the glacial samples archive strong influences of physical processes and 2) the particles from the humid climates document signals of chemical weathering. We further compared the grain morphology within the two glacial systems (Norway and Antarctica), by evaluating changes in both circularity and convexity at different points along the stream transect (Fig. 4). Both the measured HS Circularity (Figs. 4a and c) and Convexity (Figs. 4b and d) yielded contrasting patterns in the two glacial sites, notwithstanding the evident down-transect trends. While the HS Circularity of the medial and distal samples are higher than the sediment collected from the proximal part of the Norway system (Fig. 4a), the Antarctic sediment exhibits the opposite trend, with increased particle populations with the lower HS Circularities in the medial and distal samples (Fig. 4c). The contrasting trends are

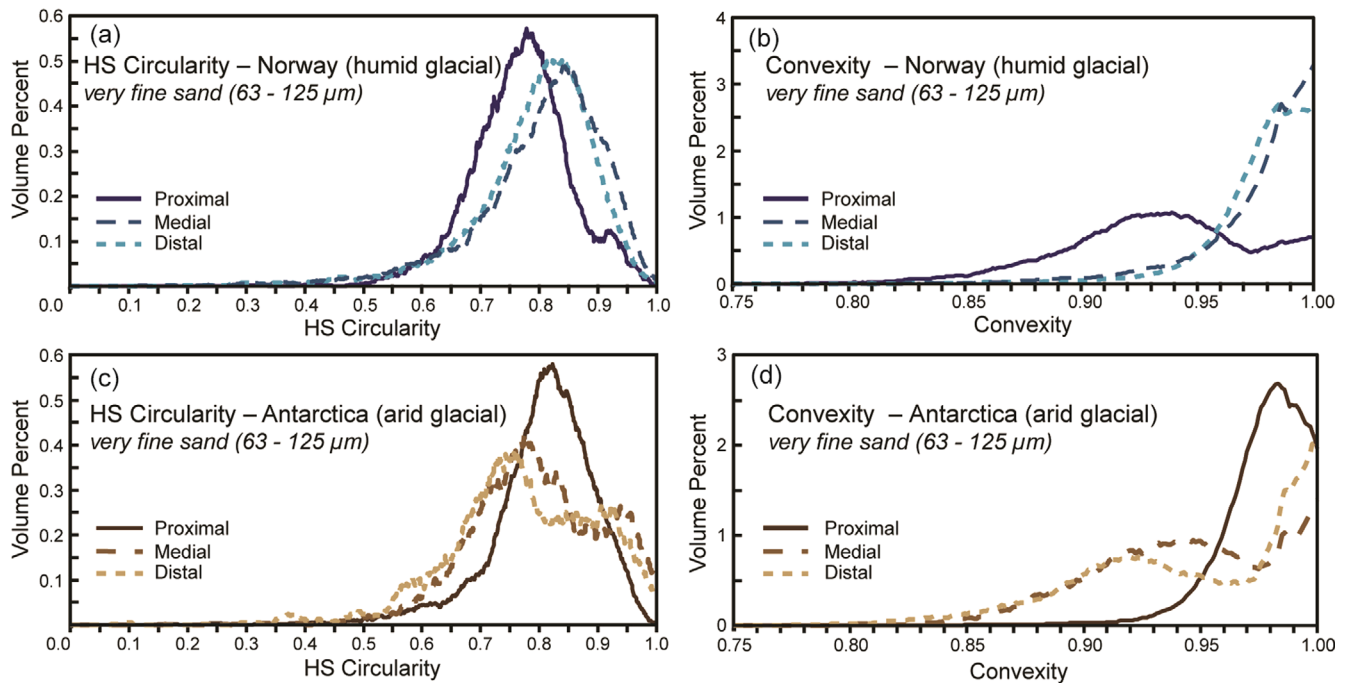


**Fig. 4.** Comparison of HS Circularity (a and c) and Convexity (b and d) measured in the humid-glacial (Norway) and arid-glacial (Antarctic) systems.

also observed in the Convexity dataset; the particles become more convex downstream in the Norway site, while the medial and distal sediments contain more spiky particles in the MDV transect (Figs. 4b and d). It is especially interesting that the particles in the proximal sample, which is least affected by fluvial processes, are least convex (mode =  $\sim 0.93$ ) in the Norway system, whereas the highest Convexity occurs in the proximal part of the MDV stream (mode =  $\sim 0.98$ ). The different initial convexity can be attributed either to the original bedrock lithology of foliated and unfoliated crystalline rocks in the Norway and MDV sites, respectively, or to differing intensities of glacial grinding and shattering underneath glaciers likely controlled by hydraulic settings of the warm- (Norway) and cold-based (MDV) glacial systems. Alternatively, eolian dust particles with higher convexity that were originally deposited on top of the glaciers by strong winds in the MDV can enter the stream during glacial melting (e.g., Marra et al., 2017). Regardless of the initial particle shape, which may not be influenced solely by the climates, the data show that climate-related processes operating in the fluvial systems improve the HS Circularity and Convexity in the wet-glacial climate and whereas the same metrics deteriorate in the dry-glacial climate. Considering that the sampling transects are located in the proximal area of the entire watersheds, drastic changes in the Convexity occurring in relatively short distances – about half of the total transects – is remarkable. Moreover, the Convexity does not change substantially between the medial and distal samples, suggesting that the fluvial sediment Convexity is readily determined in the very proximal parts of streams. The

sediment particles are physically abraded sufficiently to remove surface irregularities while being transported in the perennial stream with fast flow rates, especially during the high meltwater discharge in spring and summer.

The most prominent feature of the results from Antarctica is the shift from unimodal-like to bimodal or multimodal distributions of both parameters occurring between the proximal and medial samples (Figs. 4c and d). Similar to the Norway samples, the HS Circularity (mode =  $\sim 0.83$ ) and Convexity (mode =  $\sim 0.98$ ) of the proximal sediment are distinguished from the medial and distal samples, while the latter two display similar ranges of the shape parameters (Figs. 4c and d). The appearance and increase of particles with the higher HS Circularity ( $> 0.9$ ) and Convexity ( $> 0.98$ ) in the medial and distal MDV sediments can be accounted for the hydraulic abrasion that smooths the surfaces of the particles in the stream, similar to the Norway proglacial system. Meanwhile, the occurrence of particles with the lower HS Circularity ( $\sim 0.7\text{--}0.8$ ) and Convexity ( $\sim 0.93$ ) in the medial and distal samples (Figs. 4c and d) can be interpreted to be linked to the enhanced grain-to-grain contact and generation of surface features, such as concave-convex, groove, and upturned plates, likely due to the strong wind gusts in the MDV (Smith et al., 2018). Additionally, the insolation-induced, thermal weathering known to operate on the surficial environment of Antarctica (Hall and André, 2003; Hall et al., 2008) can further promote shattering and fracturing of the particles, lowering their HS Circularity and Convexity.

#### 4. SUMMARY

This study applied the new automated image analysis available in Morphologi G3 to the natural sediment samples from modern fluvial systems representing four extreme climate conditions (hot-arid Anza Borrego Desert of California, hot-humid Puerto Rico, glacial-arid McMurdo Dry Valleys, glacial-humid Norway) and yielded a dataset illustrating morphological differences likely owing to their varying climate conditions. Comparison of the HS Circularity of sediment particles from the four end-member climates indicates that the very fine sand fractions reflect differential physical abrasion and transport processes, whereas the morphology of the mud fraction seemingly imprints processes more related to chemical weathering. The sediments from the two glacial systems of Norway and Antarctica were further analyzed on the basis of their HS Circularity and Convexity with additional consideration for the impacts of the transport distances. While there appears to be an initial morphological difference between the two sites produced by differential hydraulic settings and eolian inputs, along with the bedrock lithology, the contrasting down-transect trends of increasing and decreasing surface irregularities were observed in the Antarctica and Norway sites, respectively. We interpret that the differing moisture availability and the strong winds in the Antarctic site likely account for the observed morphological differences. Although further work on method development and the relationship between the classic, microscope-based surface features and the parameters available in the Morphologi G3 system is required, this study successfully demonstrates the potential applicability of the image analysis to climate interpretation based on particle shapes of modern and possibly deep-time depositional systems.

#### ACKNOWLEDGMENTS

Funding for this research was provided by NSF EAR-1225162, EAR-1418716, and EAR-1543344. Y.J. Joo was financially supported by NRF PN18090 while writing this manuscript. We thank Josemar Castillo (Malvern Instruments) for technical advice. A. Soreghan thanks Dr. M. Libault and Mrs. D. Hill (Norman High School) for allowing her this opportunity. Sediment samples were collected by F. Colon, M. Elwood Madden, Y.J. Joo, K. Marra, C. Smith, G. Soreghan, A. Stumpf, and A. Velez.

#### REFERENCES

- Becker, L.W.M., Hjelstuen, B.O., Støren, E.W.N., Sejrup, H.P., and Lancaster N., 2018, Automated counting of sand-sized particles in marine records. *Sedimentology*, 65, 842–850.
- Clow, G.D., McKay, C.P., Simmons, Jr. G.M., and Wharton, Jr. R.A., 1988, Climatological observations and predicted sublimation rates at Lake Hoare, Antarctica. *Journal of Climate*, 1, 715–728.
- Doran, P.T., McKay, C.P., Fountain, A.G., Nysten, T., McKnight, D.M., Jaros, C., and Barrett, J.E., 2008, Hydrologic response to extreme warm and cold summers in the McMurdo Dry Valleys, East Antarctica. *Antarctic Science*, 20, 49–509.
- Evans, D., Phillips, E., Hiemstra, J., and Auton, C., 2006, Subglacial till: formation, sedimentary characteristics and classification. *Earth-Science Reviews*, 78, 115–176.
- Gooseff, M.N., McKnight, D.M., Doran, P., Fountain, A.G., and Lyons, W.B., 2011, Hydrological connectivity of the landscape of the McMurdo Dry Valleys, Antarctica. *Geography Compass*, 5, 666–681.
- Hall, B.L. and Denton, G.H., 2005, Surficial geology and geomorphology of eastern and central Wright Valley, Antarctica. *Geomorphology*, 64, 25–65.
- Hall, K. and André, M.F., 2003, Rock thermal data at the grain scale: applicability to granular disintegration in cold environments. *Earth Surface Processes and Landforms*, 28, 823–836.
- Hall, K., Guglielmin, M., and Strini, A., 2008, Weathering of granite in Antarctica: II. Thermal stress at the grain scale. *Earth Surface Processes and Landforms*, 33, 475–493.
- Joo, Y.J., Elwood Madden, M.E., and Soreghan, G.S., 2016, Chemical and physical weathering in a hot-arid, tectonically active alluvial system of Anza Borrego Desert, California. *Sedimentology*, 63, 1065–1083.
- Lewis, A.R., Marchant, D.R., Kowalewski, D.E., Baldwin, S.L., and Webb, L.E., 2006, The age and origin of the Labyrinth, western Dry Valleys, Antarctica: evidence for extensive middle Miocene subglacial floods and freshwater discharge to the Southern Ocean. *Geology*, 34, 513–516.
- Lutro, O. and Tveten, E., 1996, Geological map of Norway, berggrunskart Årdal M 1: 250,000. Geological Survey of Norway, Trondheim.
- Mahaney, W.C., 1995, Pleistocene and Holocene glacier thicknesses, transport histories and dynamics inferred from SEM microtextures on quartz particles. *Boreas*, 24, 293–304.
- Mahaney, W.C., 2002, Atlas of sand grain surface textures and applications. Oxford University Press, Oxford, 256 p.
- Malvern Instruments Ltd., 2015, Morphologi G3 user manual. Worcestershire, 268 p.
- Margolis, S.V. and Krinsley, D.H., 1974, Processes of formation and environmental occurrence of microfeatures on detrital quartz grains. *American Journal of Science*, 274, 449–464.
- Marra, K.R., Elwood Madden, M.E., Soreghan, G.S., and Hall, B.L., 2017, Chemical weathering trends in fine-grained ephemeral stream sediments of the McMurdo Dry Valleys, Antarctica. *Geomorphology*, 281, 13–30.
- Marra, K.R., Soreghan, G.S., Elwood Madden, M.E., Keiser, L.J., and Hall, B.L., 2014, Trends in grain size and BET surface area in cold-arid versus warm-semiarid fluvial systems. *Geomorphology*, 206, 483–491.
- May, R.W., 1980, The formation and significance of irregularly shaped quartz grains in till. *Sedimentology*, 27, 325–331.
- Pye, K. and Mazzullo, J., 1994, Effects of tropical weathering on quartz grain shape: an example from northeastern Australia. *Journal of*

- Sedimentary Research, 64, 500–507.
- Remeika, P. and Lindsay, L., 1992, Geology of Anza-Borrego: edge of creation. Sunbelt Publications, San Diego, 208 p.
- Rogers, C., Cram, C., Pease, Jr. M., and Tischler, M., 1979, Geologic map of the Yabucoa and Punta Tuna quadrangles, Puerto Rico. U.S. Geological Survey Miscellaneous Geologic Investigations Map I, San Diego, USA.
- Smith, C., Soreghan, G.S., and Ohta, T., 2018, Scanning electron microscope (SEM) microtextural analysis as a paleoclimate tool for fluvial deposits: a modern test. Geological Society of America Bulletin. <https://doi.org/10.1130/B31692.1>
- Strand, R.G., 1962, Geologic Map of California: San Diego-El Centro Sheet. California Division of Mines and Geology.
- Vos, K., Vandenberghe, N., and Elsen, J., 2014, Surface textural analysis of quartz grains by scanning electron microscopy (SEM): from sample preparation to environmental interpretation. Earth-Science Reviews, 128, 93–104.
- Woronko, B., 2016, Frost weathering versus glacial grinding in the micromorphology of quartz sand grains: processes and geological implications. Sedimentary Geology 335, 103–119.